

# DESIGN AND IMPLEMENTATION OF BIDIRECTIONAL CONVERTER FOR ELECTRIC AND HYBRID ELECTRIC VEHICLES

SASIKUMAR S<sup>1</sup>,

1 Research Scholar, Department of Electrical Engineering, Sona college of Technology,  
Address: 10/4, Anna Nagar, Bharathi Dasan Salai, Rasipuram, Namakkal District, Pin No. : 637408.  
Mobile No. : +91\_944-3515-404, Email ID: Sasikumar.eee786@gmail.com,

KRISHNAMOORTHY K<sup>2</sup>

2 Associate Professor, Department of Electrical Engineering, Sona college of Technology,  
Address: 10/4, Anna Nagar, Bharathi Dasan Salai, Rasipuram, Namakkal District, Pin No. : 637408.  
Mobile No. : +91\_944-3515-404, Email ID: krishrevathii25@gmail.com

## ABSTRACT

*Nowadays, the power demand and a shortage of fuel considered as one of the most critical worldwide issues, power, and costly fuel becomes a significant challenge for customers. This research designs a bidirectional converter (BC) following the trend has seen for renewable energy sources like photovoltaic, and, wind. This BC is proposed to transfer power from grid/ renewable energy systems to the electric vehicle system (EVS) as well as EVS to grid power transfer. The proposed work of dual stage topology allows maintaining input voltage as well as output voltage level. During discharging, the energy from a battery pack returned to the grid where the dc link bus will interconnect with electric traction inverter. Depending upon power demand, the converter input and the output voltage can be used to set reference voltage. A fuzzy proportional integral controller (FPIC) is used to regulate the voltage of dc link capacitor. The performance of the proposed BC regarding voltage gain, efficiency, and the flexible application has been analyzed using MATLAB simulation and also with experimental studies.*

**Keywords-** Bi-directional converter, Cascade buck-boost converter, fuzzy propagation integral controller, an electric vehicle battery storage system to grid power transfer

## I. INTRODUCTION

Nowadays, the pollution from global warming effects and cost of fuel are increasing significantly. Switching to use renewable energy and

electric vehicles are some prospective ways that can solve these problems. The electric vehicles are becoming a popular choice to use instead of internal combustion vehicles especially in the last ten years [1]. Many leading vehicles manufactures in the world have a high competition to produce and sell the electric vehicles under their brand to domestic and international market. [2] Write that the electric vehicles could be the important one in the transport sector in the future. During the last few decades, the adoption of using Electric Vehicles is continuously increasing due to some reasons. Their performance is improving; they have a smaller environmental impact with no greenhouse emissions while their efficiency begins to outperform traditional fossil fuel vehicles. Therefore, many governments and organizations in the world have launched the policy to support the electric vehicles in their countries.

However, electric vehicles charging stations which are the essential elements of electric vehicles have not widespread yet. The main reason for this is that of electric vehicles charging stations not only increase the electrical grid demand but also increases the emission from petroleum-electrical generation. The grid source is not the best solution for charging the electric vehicles [3-5]. Due to the improving ability and performance of the electric vehicles are charging by using renewable energy resources instead of grid-source should be integrated into their systems as well. These will also have the added benefit of making EV with greener credentials as their environmental impact depends upon the primary source of energy.

The most of the existing systems have used to analyze in open loop methodology; they did not analyze their converter with proper loads, [6-8] So that we cannot be able to predict the efficiency and performance in this state. Some of them have analyzed with closed loop system, but they had not utilized modern controllers and efficient mode conversions. So their converters are facing more problems like switching losses, harmonics, and, complexity. The primary goal of the research is to allow active participation of electric vehicles in power systems with renewable energy sources. Presently, it deals with the design and control implementation of a BC, Fig. 1. showing the configuration of BC. It achieves the power transfer between the EVS and grid. Compared with other converters, the proposed converter has more efficiency and reliability in this category as well as this design is a simple structure with less number of components. The developed converter consists of four switches integrated with a couple of inductors. An ultra-capacitor placed in the center of switches that act as an intermittent stage. However, the presented BC topology allows individual stage modules of both interleaved input and output.

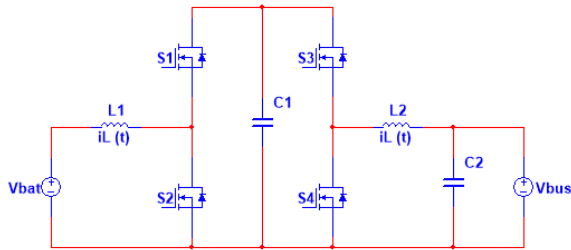


Fig. 1. Proposed circuit topology of BC

## 2. EVS TO GRID POWER EXCHANGE

The BC is part of the EVS that manage power flow between the battery pack and the grid through dc bus; when excessive power is available in the system, the battery discharging energy into the dc bus power line. The BC is operated in two modes, i.e., step up and step down with a maximum range of voltage is achieved in both input and output sides. It allows the access of multi-input and multi-output. So, the converter topology is more flexible to transfer the excess power of electric vehicle battery storage system into the dc bus grid. So, that can sustain from power demand bitterly compared to the other existing methods. This converter performs dual modes in both directions; one is a buck, and another one is boost operation.

## 3. BIDIRECTIONAL BUCK BOOST CONVERTER

### a) Control of BC

In this section, the design of the bidirectional buck-boost converter using metal–oxide–semiconductor field-effect transistor (MOSFET) and also controller topology of a proposed converter is discuss below.

This proposed BC is a significant unit in electric vehicles for power managing between EVS and the grid. According to the need, power transfer achieved in either direction. Fig. 1. Shows the detailed data's of proposed converter, where the converter called a non-isolated bidirectional converter with ultra-capacitor (NIBCUC). It consists of two stages that should interconnect with DC link capacitor for smooth power flow in both input and output side. Those stages controlled by using an individual controller for each stage. So that, we can achieve high-efficiency operation through this topology and also it reduces voltage stress, auxiliary components in this topology.

The desired operations of both stages are acting as the two different modes using individual controller unit of each stage, and they are buck mode and boost mode. While the power level is regret below the nominal level of the system means, this proposed converter operates as a boost converter as well as the power level is regret above the nominal level of the system means, this proposed converter operates as a buck converter. However, the proposed converter can be able to operate in dual modes in both input and output side. The dc stages on both input and output sides have interconnected through intermediate storage unit of dc link capacitor. The detailed operation of BC in stage wise is describing in below, during the power transfer from the EVS to the grid, stage one operated as a boost converter, and stage two operated as a buck converter. During the power transfer from the grid to EVS, the operation of converter mode is similar to EVS to the grid, which means stage two operated as a boost converter and stage one operated as a buck converter. These can utilize the control of power flow in any given direction. When the direction of power flow is changed as our requirement by turn off pulse width modulation (PWM) signal in the controller as well as it waits to reach zero of the inductor current, After

that controller considered next command as a new control command. The voltage of intermediate storage unit dc link capacitor and dc bus voltage regulated by using separate FPIC. According to the charge and load unit of battery, the nominal voltage of dc link capacitor has adjusted.

#### b) BC Configuration of components sizing

A configuration of half- bridge switch topology is reducing the switching stresses compared to other existing topologies. Higher frequency switching minimizes the reactive components sizing. Then inductor size depends upon allowable ripple in inductor current as well as capacitor size is determined based on which allows ripple in the voltage of a capacitor. [9-11] the sizing relationship is;

$$\begin{aligned} L_1 &= \frac{V_{\text{batt\_max}} D_{1\_max} T}{\Delta I_{L1}} \\ L_2 &= \frac{(V_{c1\_max} - V_{c2\_min}) D_{2\_max} T}{\Delta I_{L2}} \end{aligned} \quad (1)$$

$$\begin{aligned} C_1 &= \frac{I_{L1\_max} D_{2\_max} T}{\Delta V_{c1}} \\ C_2 &= \frac{I_{L2\_max} D_{2\_max} T}{\Delta V_{c2}}. \end{aligned} \quad (2)$$

Here, T is switching period; the maximum ON time of switches S<sub>1</sub>, and S<sub>4</sub> is accessed based on D<sub>1\_max</sub>T and D<sub>2\_max</sub>T. ΔI<sub>L1</sub>, ΔI<sub>L2</sub>, ΔV<sub>c1</sub>, and ΔV<sub>c2</sub> which allow maximum ripple currents and voltages of the reactive components in a circuit. Power transfer characteristics are analyzed individually in two different modes; one is continuous conduction, and another one is discontinuous conduction. I<sub>o1</sub> is the steady-state inductor current; the power transfer equation continues conduction derived as

$$\begin{aligned} P_1 &= V_{in} I_{o1} + \frac{(V_{c1} - V_{in})^2 T V_{in}}{2 V_{c1} L_1} \\ &+ \frac{V_{in} T (V_{in} - V_{c1}) \left(1 - \frac{2 V_{in}}{V_{c1}}\right)}{2 L_1}. \end{aligned} \quad (3)$$

The derived power transfer of discontinuous conduction equation is

$$P_1 = \frac{V_{in}^2 t_1^2}{2 T L_1} - \frac{(V_{c1} - V_{in})^2 (t_2^2 - t_1^2)}{2 L_1} \quad (4)$$

$$t_2 = t_1 \sqrt{1 - \left(\frac{V_{in}}{V_{c1} - V_{in}}\right)^2}. \quad (5)$$

## 4. IMPLEMENTATION OF FPIC

#### a) Controller for BC

In a design of proposed BC, the controller takes place the central role. Nowadays, the most of the applications preferred the artificial fuzzy controller for controlling both input and output of the system. Fuzzy controllers have broad applications in power electronics field. Because this fuzzy controller control methods are elementary comparatively conventional controllers and it is conceptually easy to understand. It is more compatible to operate with any system which resembles human reasoning. So this method entirely imitates the way of human reasoning and decision making with all intermediate possibilities that help to deal with the uncertainty in the engineering field. After that, the controller can adopt both approaches; one is purely mathematical, and another one is purely logics [12-13].

The fuzzy controllers do not require any final accurate values to model in the real world, and it adapts to operate with the actual results getting from a system. The fuzzy controller can accommodate with logic and natural human language, so the controller is highly robust which provide easy to construct and understand by the users. The FPIC has more merits than the conventional controllers (i.e., PI, PD, and, PID). The proposed methods can able to process in non-linearity condition with inexplicit inputs of the systems and it describes the functions of the system in both automates conversion and intuitive methods for an understanding of both humans and machines adequately. The principal operation of proposed topology is used to control voltage and current on either side. The proposed BC system investigated with loads, and it verified through MATLAB- Simulink software (i.e., simulation) and experimental setup. A block diagram of FPIC shown in Fig. 2.

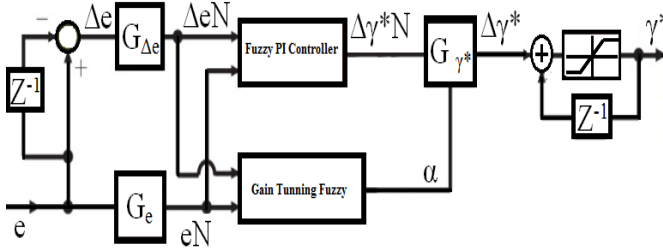


Fig. 2. Block diagram of FPIC system

A “fuzzy propagation integral controller” is merging of both fuzzy and conventional propagation integral (PI) controllers. The primary goal of a controller is to maintain desired output voltage on either side. Those PI parameters are fine-tuned dynamically with fuzzy controllers to control the output voltage as well as intermediate stage voltage. This composed controller has two scale factors  $G_e$  and the input  $G_{\Delta e}$ . Both error ( $eN$ ) and error change ( $\Delta eN$ ) are the inputs of the fuzzy controller; their outputs represent concerning proportional gain  $K_p$  as well as integral time  $T_i$ . The fuzzy controllers can adjust the values in real time with these parameters  $K_p$  and  $T_i$ . The interval of  $[K_p, \min, K_p, \max]$  has limited gain  $K_p$  within it, which determined in simulations. For our convenience,  $K_p$  is typically accessed in between zero to one through the following transformation.

$$K_p' = K_p - K_p, \min K_p, \max - K_p, \min \quad (6)$$

Then, the value of  $K_p'$  represents normalized output value of fuzzy controller, then we get  $K_p$  as;

$$K_p = (K_p, \min - K_p, \max) K_p' + K_p, \min \quad (7)$$

However, during the interval  $[0, K_p, \max]$  to set the proportional gain values in different reference values,

$$K_p = K_p, \max K_p' \quad (8)$$

The input and output tables for fuzzy logic shown below. The details of the variation made on t.

#### b) FPIC Membership functions of a system

The Membership functions for FPIC controller is pointed out in Fig. 3. “ $\Delta e$ ,  $\Delta eN$ ” are input variables of the Membership functions and “ $\Delta \gamma * N$ ” is the normalized output variable are in the closed interval of  $[-1, 1]$ . The Membership functions for gain tuned fuzzy controllers concerning input and

output variables show in Fig. 3 (a) and 3 (b). In the closed interval of  $[-1, 1]$ , Input variables “ $\Delta e$  N  $\Delta eN$ ” defined, and similarly, the closed interval of  $[0, 1]$  the output variable “ $\alpha$ ” defined within the interval. The error and change in error are the inputs of Mamdani based fuzzy interference system. Most of the membership function variables have triangular shapes as shown in Fig. 3 and the trapezoidal excluded in extreme condition, and neighboring functions are overlapping with fifty percent. The linguistic variables used in the member functions are Negative Large (NL), Negative Medium (NM), Negative Small (NS), Zero (ZE), Positive Small (PS), Positive Medium (PM), and Positive Large (PL) and so on. The rule-based membership functions are shown Table I and II.

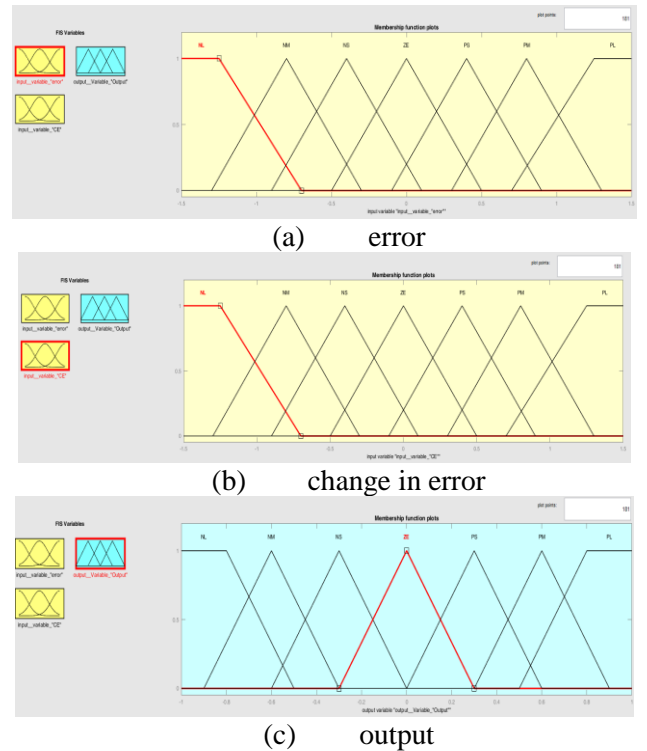


Fig. 3. (a-c) FPIC Membership function plots of a system

#### c) Scaling factors and Rule bases:

The two inputs of scaling factor are “ $G_{\Delta e}$ ,  $G_e$ ” and the output of scaling factor is “ $G_{\gamma *}$ ” can be adjusted dynamically through updating of the scaling factor “ $\alpha$ .” The independent rule-based fuzzy model “e,  $\Delta e$ ” computed in online with “ $\alpha$ .” Then the relationship between scaling factor and the input as well as output variables of the self- tuned FPIC is derived and given below:

$$e_N = G \cdot e \cdot e \quad (9)$$

$$\Delta e_N = G \Delta e \cdot \Delta e \quad (10)$$

$$\Delta \gamma^* = (\alpha \cdot G \gamma^*) \cdot \Delta \gamma_N^* \quad (11)$$

In the Rule bases, the incremental changes in the output of the controller are  $\Delta \gamma_N^*$  to FPIC is determined by the following rules:

$$R_x : \text{if } e_N \text{ is } E \text{ and } \Delta e_N \text{ is } \Delta E \text{ then } \Delta \gamma_N^* \text{ is } \Delta \Gamma_N^* \quad (12)$$

Where  $e = \Delta e = \Delta \gamma_N^* = \{NL, NM, NS, ZE, PS, PM, PL\}$ . The gain tuned the following rules determine fuzzy controller output of " $\alpha$ ":

$$R_x : \text{if } e_N \text{ is } E \text{ and } \Delta e_N \text{ is } \Delta E \text{ then } \alpha \text{ is } \chi \quad (13)$$

Where  $e = \Delta e = \{NL, NM, NS, ZE, PS, PM, PL\}$  and  $\chi = \{ZE, VS, S, SL, ML, L, VB\}$ . The rule base for  $\Delta \gamma_N^*$  and " $\alpha$ " is shown in both table 1 and 2 respectively.

The purpose of the gain tuned fuzzy controller is updated continuously on each sample time into the computational value of " $\alpha$ ." The output percentage of scaling factor " $G \gamma^*$ ," which is controlled by the computational output of " $\alpha$ " and " $\Delta \gamma^*$ " is determined for calculation of new samples. The gain tuned fuzzy controller rules are based on knowledge and precision of the proposed BC to avoid large undershoot as well as overshoot by using the direct torque control (DTC) type control. Then the defuzzification operations are performed by the center of gravity methodology.

TABLE I  
Rule base computation of  $\Delta \gamma_N^*$  for FPIC

$\Delta e/e$	NL	NM	NS	ZE	PS	PM	PL
NL	NL	NL	NL	NL	NM	NS	ZE
NM	NL	NL	NL	NM	NS	ZE	PS
NS	NL	NL	NM	NS	ZE	PS	PS
ZE	NL	NM	NS	ZE	ZE	PM	PM
PS	NM	NS	ZE	PS	PS	PL	PL
PM	NS	ZE	PS	PM	PM	PL	PL
PL	ZE	PS	PS	PM	PL	PL	PL

TABLE II  
Rule base computation of  $\alpha$  for FPIC

$\Delta e/e$	NL	NM	NS	ZE	PS	PM	PL
NL	VB	VB	VB	L	SL	S	ZE
NM	VB	VB	L	L	ML	S	VS
NS	VB	ML	L	VB	VS	S	VS
ZE	S	SL	ML	ZE	ML	SL	S
PS	VS	S	VS	VB	L	ML	VB
PM	VS	S	ML	L	L	VB	VB
PL	ZE	S	SL	L	VB	VB	VB

## 5. SIMULATION RESULTS

The proposed BC simulations are carried out in MATLAB- Simulink model. The proposed techniques analyzed with both conventional and non-conventional controllers. The efficiency is evaluated based on peak time [ $T_s$  (s)], settling time [ $T_p$  (s)], rise time [ $T_r$  (s)] and steady-state error [ $E_{ss}$  (v)]. These systems used a DC machine and BLDC motor as a load.

In conventional controllers, a proportional integral control technique has simulated with BC. Which can provide the output but it has attained more losses, where the output performances in buck and boost modes given in Table III. These table results have obtained and validated in the laboratory using MATLAB- Simulink.

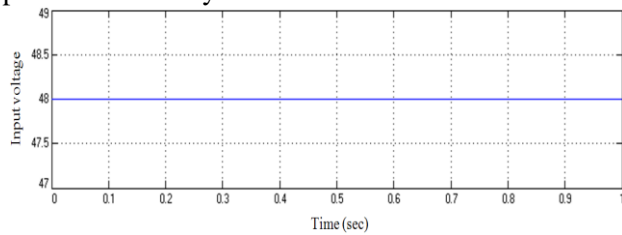
Table III: Performances of controllers in buck/boost mode

Controllers	Rise time $T_r$ (s)	Peak time $T_s$ (s)	Settling time $T_p$ (s)	Steady state error $E_{ss}$ (Volts)
PI controller(Buck)	0.08	1.2	0.78	0.9
Proposed FPIC(Buck)	0.02	0.0	0.0	0.0
PI controller(Boost)	0.05	0.81	0.53	0.8
Proposed FPIC(Boost)	0.02	0.04	0.22	0.1

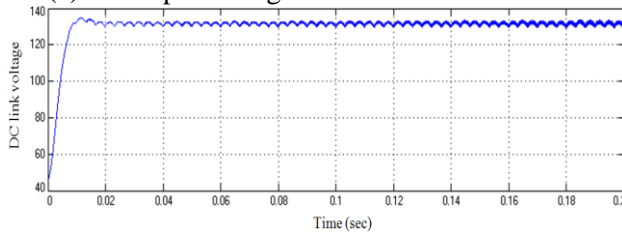
In Boost mode, the rise time of PI enhanced BC is 0.05 and peak time is 0.81 secs. Then the

settling time of the output is 0.53, and steady-state error is 0.8 volts. Then the output performance in buck mode is shown the followed details. The rise time of PI enhanced BC is 0.08 and peak time is 1.2. Then the settling time of the output is 0.78, and steady-state error is 0.9 volts. In the same way, the non-conventional controller (i.e., FPIC) enhanced with proposed BC. In boost mode, the rise time is 0.02 and peak time is 0.04. The settling time of this system is 0.22 as well as the steady-state error is 0.1 volts. In buck mode, the rise time is 0.02 and peak time, settling time of this system as well as the steady-state error is nil (i.e., almost equivalent to zero). So, we can analyze the performance and efficiency of these results. The FPIC is more efficient than PI controller. Both the losses and time delay has sustained in an inappropriate level of the BC output. So this FPIC Integrated BC is analyzed with BLDC motor as a load. So further we can know the prominent state of this converter in specific load condition.

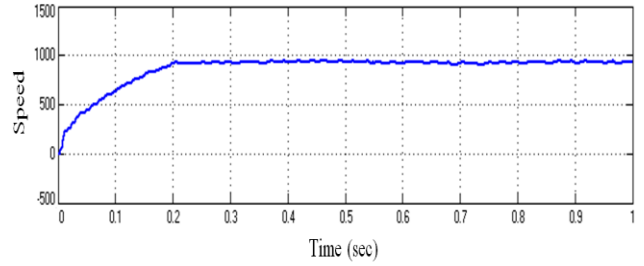
This system considers the torque, rotor speed, output power torque ripple and total harmonic distortion. While increasing the input voltage is undoubtedly improving the efficiency level saturation, as well as load increases gradually reduces the efficiency level. The losses of the proposed system are comparatively low with the existing methods. Then the torque is 14.98 Nm, the rotor speed is 962.4 rad/s. Where the output power of the system is 592.1 Watts, and the torque ripple in the load is 1.4 Nm. The total harmonic distortion of the proposed system has achieved the value of 30.75 percent efficiently. The Simulink results show below



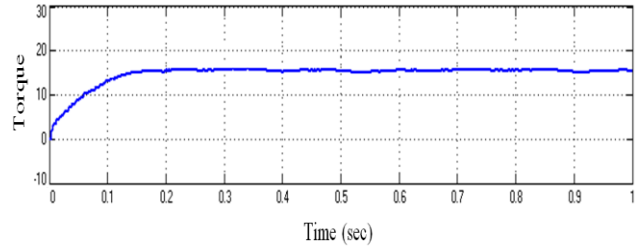
(a) The input voltage of NIBCUC with BLDC



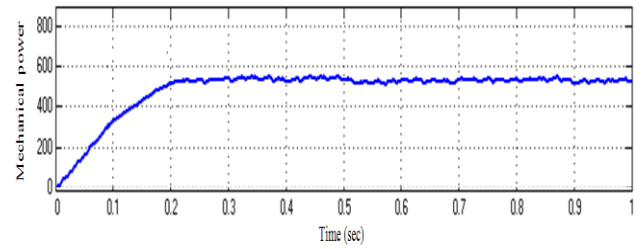
(b) DC link voltage of NIBCUC with BLDC



(c) The speed of BLDC motor

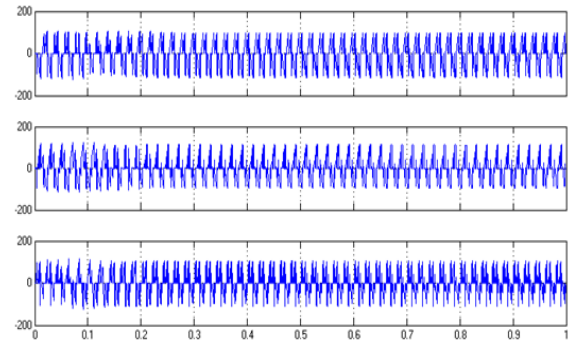


(d) The torque of BLDC motor

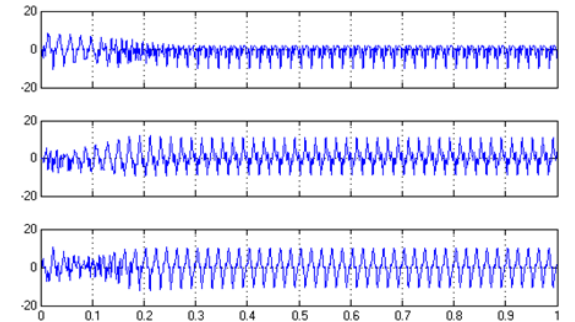


(e) Mechanical power of BLDC motor

Fig. 4. (a-e) The results of NIBCUC with BLDC motor



(a) Inverter output voltage of NIBCUC with BLDC motor as a load



(b) Inverter output current of NIBCUC with BLDC motor as a load



Fig. 5. (a) Inverter output voltage and (b) Inverter output current

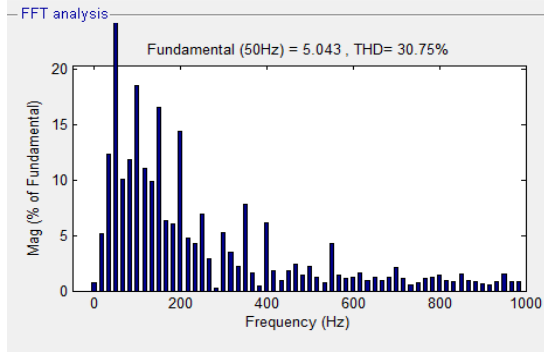


Fig. 6. THD%

## 6. EXPERIMENTAL RESULTS

The proposed BC performance is verified with the prototype model as shown in Fig. 7(a), where 25/50-V prototype model built in the laboratory. The parameters used in the circuit given in Table IV.

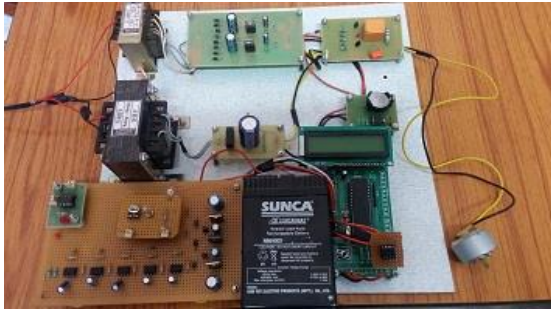


Fig. 7(a). A prototype model of BC

Table IV. Experimental Parameters

Parameter	Value
Rated Low Voltage	25V
Rated high Voltage	50V
MOSFET IRF3710	$V_{DSS} = 100\text{ V}$ , $R_{DS(ON)} = 0.025\Omega$ , and $I_D = 57\text{ A}$
Capacitor	$10\mu\text{F}$
Switching Frequency	50 Hz

Figure 7(b) shown the input voltage of prototype model as well as the dynamic responses of the BC in both buck and boost mode as shown in Figure 7(c) and 7(d). In Figure .8(a) - 8(c) shows the switching pulses of the switches, which generated by using a controller.

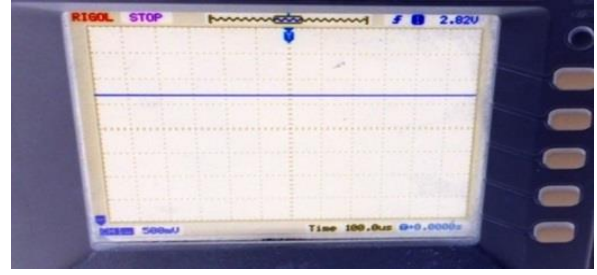


Fig. 7(b). Input Voltage

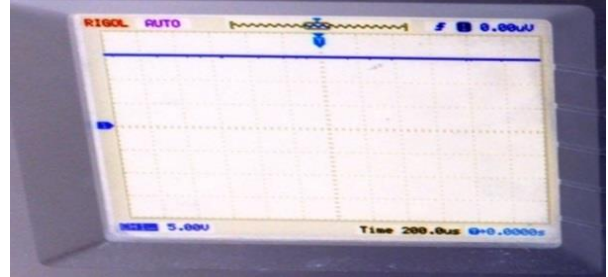


Fig.7(c). Output Voltage for Boost Mode

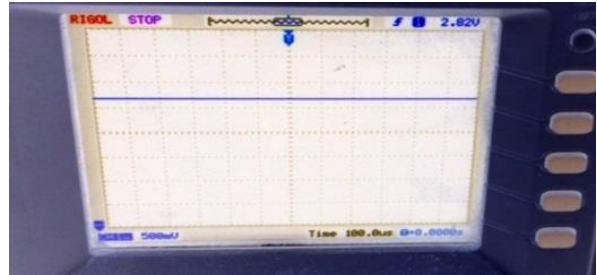


Fig.7(d). Output Voltage for Buck Mode

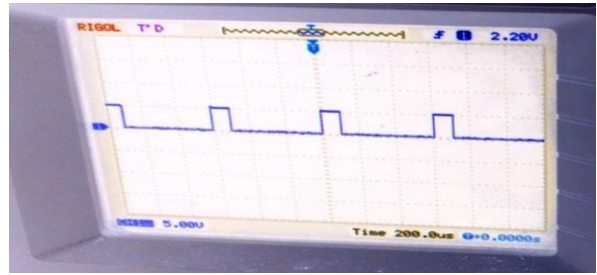


Fig.8(a): Switching Pulse for Switches in FPIC (5V)

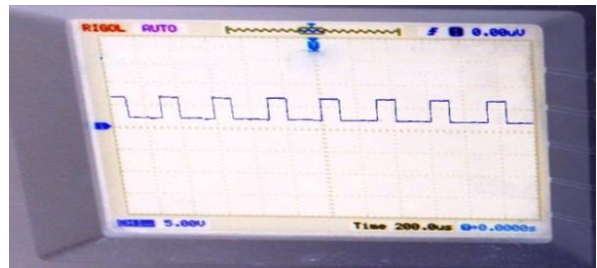


Fig.8(b): Switching Pulse for Driver Output Pulse (10V)

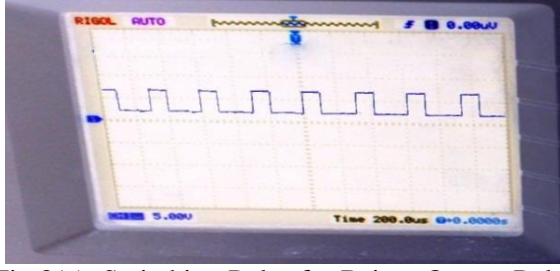


Fig.8(c): Switching Pulse for Driver Output Pulse (10V)

According to the Figure 9, the voltage stress on the switches (S1 and S2) is equal to  $(V_H + V_L)/2$ . Also, the voltage stress on the switches (S3 and S4) equals to  $(V_H + V_L)$ .

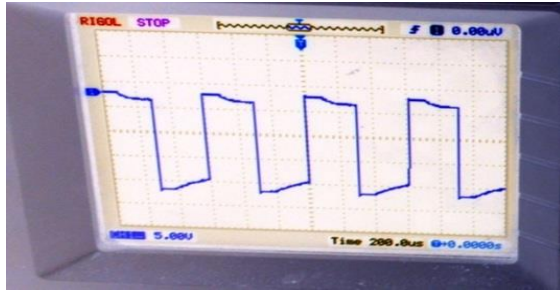


Fig.9. Across voltage of the switches.

The efficiency defined as the ratio of output power and input power of the system where it is expressed as;

$$\eta = (P_{out} / P_{in}) \quad (14)$$

The power wastages also calculated and expressed as;

$$P_{waste} = P_{in} - P_{out} \quad (15)$$

Table V Performances of controllers in buck/boost mode in the prototype model

Controllers	Mode	Efficiency
PI	Boost	90%
	Buck	84%
Proposed FPIC	Boost	94.7%
	Buck	90.4%

The measured efficiency of the proposed FPIC and the PI-based BC tabulated in Table V. At full-load condition, the efficiency of the FPIC controlled BC is 94.7% in boost mode and is 90.4% in buck mode. As well as, the efficiency of the PI

controlled BC is 90% in boost mode and is 84% in buck mode. Hence, to clarify that the efficiency of the proposed FPIC converter is higher than the conventional PI bidirectional boost/buck converter. As per the results, the output of experimental studies is slightly varied from simulation results. However, the efficiency of BC in both simulation and experimental studied is almost equalling, which are very clear from the results we obtained.

## 7. CONCLUSION

The proposed bidirectional buck-boost converter using fuzzy proportional integral controller topology is more suitable for electric / hybrid vehicles as well as high power applications with low switching losses. Due to the cascade method with the individual controller for either stage make this converter more flexible and also improves efficiency and performances, which shown in results. This proposed methodology is not only accomplished the charging, but it also transfers the power to the grid through dc link bus. Apart from that, this method is reducing the complexity as well as the expense of the circuit. This circuit validated with both PI and FPIC controllers using MATLAB Simulink as well as experimental setup, as per the values obtained in the results. The FPIC is more efficient and adaptable to the proposed BC.

## REFERENCES

- [1] Stuart Speidel and Thomas Bräunl, "Driving and charging patterns of electric vehicles for energy usage", Renewable and Sustainable Energy Reviews, vol. 40, issue C, pages 97-110, 2014.
- [2] Azadfar, E., Sreeram, V., Harries, D., 'The investigation of the major factors influencing plug-in electric vehicle driving patterns and charging behavior', Renewable & Sustainable Energy Reviews, 42, pp. 1065-1076, 2015.
- [3] M. Vasiladioties, A. Rufer, "A modular multiport power electronic transformer with integrated split battery energy storage for versatile ultrafast EV charging stations," IEEE Trans. Ind. Electron., vol. 62, no. 5, pp. 3213-3222, May 2015.
- [4] Mehnaz Akhter khan, Iqbal Husain, Yilmaz Sozer," A Bidirectional DC-DC Converter With Overlapping Input and Output Voltage Ranges and Vehicle to Grid Energy Transfer Capability",



IEEE Journal of emerging and selected topics in power electronics, VOL. 2, NO. Three September 2014, pp. 507-516.

- [5] T. Mishima, K. Akamatsu, and M. Nakaoka, "A high frequency-link secondary-side phase-shifted full-range soft-switching PWM DC-DC converter with ZCS active rectifier for EV battery chargers," IEEE Trans. Power Electron., vol. 28, no. 12, pp. 5758–5773, Dec. 2013.
- [6] B. Gu, J.-S. Lai, N. Kees, and C. Zheng, "Hybrid-switching full-bridge DC-DC converter with minimal voltage stress of bridge rectifier, reduced circulating losses, and filter requirement for electric vehicle battery chargers," IEEE Trans. Power Electron., vol. 28, no. 3, pp. 1132–1144, Mar. 2013.
- [7] A. Ahmed, M. A. Khan, M. Badawy, Y. Sozer, and I. Husain, "Performance analysis of Bi-directional DC-DC Converters for electric vehicles and charging infrastructure," in Proc. IEEE ECCE, pp. 1401–1408, Sep. 2013.
- [8] S. Njoya Motapon, L.-A. Dessaint, and K. Al-Haddad, "A comparative study of energy management schemes for a fuel cell hybrid emergency power system of more electric aircraft," IEEE Trans. Ind. Electron., vol. 61, no. 3, pp. 1320–1334, Mar. 2014.
- [9] J.-H. Lee, D.-H. Yu, J.-G. Kim, Y.-H. Kim, D.-Y. Jung, Y.-C. Jung and C.-Y. Won, "Auxiliary switch control of a bidirectional soft-switching DC-DC converter," IEEE Trans. Power Electron., vol. 28, no. 12, pp. 5446-5457, Dec. 2013.
- [10] J.G. de Matos, F. S. F. e Silva, L. A. de S Ribeiro, "Power control in AC isolated microgrids with renewable energy sources and energy storage systems," IEEE Trans. Ind. Electron., vol. 62, no. 6, pp. 3490-3498, June 2015.
- [11] R.-J. Wai, R.-Y. Duan, and K.-H. Jheng, "High-efficiency bidirectional dc-dc converter with high-voltage gain," IET Power Electron., vol. 5, no. 2, pp. 173–184, Apr. 2012.
- [12] Pavlovsky, Guidi, Kawamura, "Buck/Boost dc-dc Converter Topology with Soft Switching in the Whole Operating Regn."IEEE Transaction Power Electronics, vol. 29, pp.851-862, 2014.
- [13] D.-Y. Jung, S.-H. Hwang, Y.-H. Ji, J.-H. Lee, Y.-C. Jung and C.-Y. Won, "Soft-switching bidirectional DC/DC converter with a LC series

resonant circuit," IEEE Trans. Power Electron., vol. 28, no. 4, pp. 1680-1690, Apr. 2013.